Bioelectrochemistry 73 (2008) 129–136

Contents lists available at ScienceDirect

Bioelectrochemistry

journal homepage: www.elsevier.com/locate/bioelechem

Further characterization of cation channels present in the chicken red blood cell membrane

Franck Lapaix, Guillaume Bouyer, Serge Thomas, Stéphane Egée *

UMR 7150 Université Pierre and Marie Curie, CNRS Mer et Santé, Station Biologique de Roscoff Place G. Teissier 29680 Roscoff, France

ARTICLE INFO

Article history:
Received 31 May 2007
Received in revised form 4 April 2008
Accepted 7 April 2008
Available online 13 April 2008

Keywords:
Red blood cells
Ionic channels
Patch-clamp
Chicken
Cation

ABSTRACT

In this paper, we provide an update on cation channels in nucleated chicken erythrocytes. Patch-clamp techniques were used to further characterize the two different types of cation channels present in the membrane of chicken red blood. In the whole-cell mode, with Ringer in the bath and internal K^+ saline in the pipette solution, the membrane conductance was generated by cationic currents, since the reversal potential was shifted toward cations equilibrium when the impermeant cation NMDG was substituted to small cations. The membrane conductance could be increased by application of mechanical deformation or by the addition of agonists of the cAMP-dependent pathway. At the unitary level, two different types of cationic channels were revealed and could account for the cationic conductance observed in whole-cell configuration. One of them belongs to the family of stretch-activated cationic channel showing changes in activity under conditions of membrane deformation, whereas the second one belongs to the family of the cAMP activated cationic channels. These two channels could be distinguished according to their unitary conductances and drug sensitivities. The stretch-activated channel was sensitive to Gd^{3+} and the cAMP-dependent channel was sensitive to flufenamic acid. Possible role of these channels in cell volume regulation process is discussed.

1. Introduction

The membrane of healthy unstimulated red blood cell (RBC) is characterized in most species by very high permeability to Cl^- ions due to the presence of highly efficient Cl^-/HCO_3^- exchanger [1] and a low permeability to small cations. However, this membrane may become more permeable to cations in response to physiological challenge such as cell volume regulation after anisosmotic perturbation [2,3], hormonal stimulation [4], genetic disorder such as sickle cells disease [5–7] or after infection by the malaria parasite *Plasmodium* spp. [8–12]. These changes in cation permeability may occur via electroneutral transporters (KCl and NaK2Cl cotransporter [13,14] $K^+(Na^+)/H^+$ [15]or Na^+/H^+ [16] exchangers for review see [1]) or via conductive pathways such as ion channels [17]. This is particularly relevant in the context of changes in membrane permeability properties after infection by *Plasmodium* spp. Indeed, to accomplish its life cycle, the parasite needs to synthesize new membrane and to be supplemented in the phospholipid precursor choline which is present in cationic form in solution. Moreover, recent evidences are given that malaria-induced cation permeability is important for growth [18].

It is now firmly established that non-selective cation (NSC) channels are present in all erythrocytes studied so far [11,19–25]. But, whereas channels of this type have been described for a variety of preparations, the molecular identity of these channels is at present unknown.

Most of them are inhibited by the antiinflammatory drug flufenamate (10^{-4} M) as well as by gadolinium ions (Gd^{3+} 10^{-5}–10^{-3} M) and most typically, their conductance is in the range of 15–25 pS. Here we readdress the characterization of the cation channels present in the chicken RBCs. The present study extends the previous evidence showing that the chicken red blood cell membrane is endowed with two types of NSC channels. The first channel type is non-selective for monovalent cations, it is clearly sensitive to membrane deformation and inhibited by Gd^{3+}. The second type of channel described in the present paper is activated either by or via a cAMP-dependent pathway and can be distinguished from the stretch-activated NSC channels by its unitary conductance and sensitivity to flufenamic acid. Possible role of these channels in cell volume regulation processes is discussed.

2. Materials and methods

2.1. Preparation of cells

Five-week-old chickens (*Gallus domesticus*) were obtained from "La Ferme de Mezarc'han" located in Saint-Pol-de-Leon (Brittany, France), held indoors and allowed access to diet and water ad libitum. Diet was a standard commercial corn-soybean meal ration. The chickens were anesthetized with chloroform, and blood samples were drawn by cardiac puncture using 18 gauge needle and heparinized syringe. The blood cells were washed three times in isotonic saline solution (Ringer

* Corresponding author. Tel.: +33 298 29 23 82; fax: +33 298 29 23 10.
E-mail address: egee@sb-roscoff.fr (S. Egée).

1567-5394/$ – see front matter © 2008 Elsevier B.V. All rights reserved.
doi:10.1016/j.bioelechem.2008.04.003

Table 1

Composition of the bathing solutions

	Ringer Na	K_{int}	Na_{int}	K_{int} 1/2	NMDG
	pCa3	pCa8	pCa8	pCa8	pCa8
NaCl	145	–	145	–	–
KCl	5	145	–	72.5	–
$MgCl_2$	–	1.22	1.22	1.22	1.22
$MgSO_4$	1	–	–	–	–
$CaCl_2$	1.4	0.29	0.29	0.29	0.29
Hepes	10	–	–	–	–
Hepes/tris	–	10	10	10	10
EGTA	–	5	5	5	5
D-glucose	10	10			
NMDG	–	–	–	–	145
pH	7.40	7.20	7.20	7.20	7.20

Composition of the pipette solutions

	KCl	NaCl	K gluconate
	pCa3	pCa3	pCa3
NaCl	–	145	–
KCl	145	–	–
$MgCl_2$	1.2	1.2	1.2
$CaCl_2$	1.4	1.4	1.4
K Gluconate	–	–	145
Hepes/tris	10	10	10
D-glucose	10	10	10
pH	7.40	7.40	7.40

Na^+ pCa3, ionic composition in Table 1) and the buffy coat removed by aspiration. Cells were then incubated overnight at 4 °C in the saline solution to ensure a steady state with respect to ion and water contents before experimental treatment.

2.2. Experimental solutions and drugs

The composition of solutions used in patch pipettes and bathing solutions is described in Table 1. The calcium concentration was adjusted to pCa3 in cell-attached configuration, whilst it was adjusted to pCa8 in the bathing solutions in the excised inside-out configuration and in pipette solutions in the whole-cell configuration. All solutions were equilibrated in atmospheric air and filtered through 0.2 µm Millipore cellulose disks and had a final osmolarity of 310 mosM. Flufenamic acid, cAMP, 8Br-cAMP and *N*-Methyl-D-Glucamine chloride (NMDG) were purchased from Sigma Chemical. Gadolinium chloride hexahydrate was obtained from Aldrich.

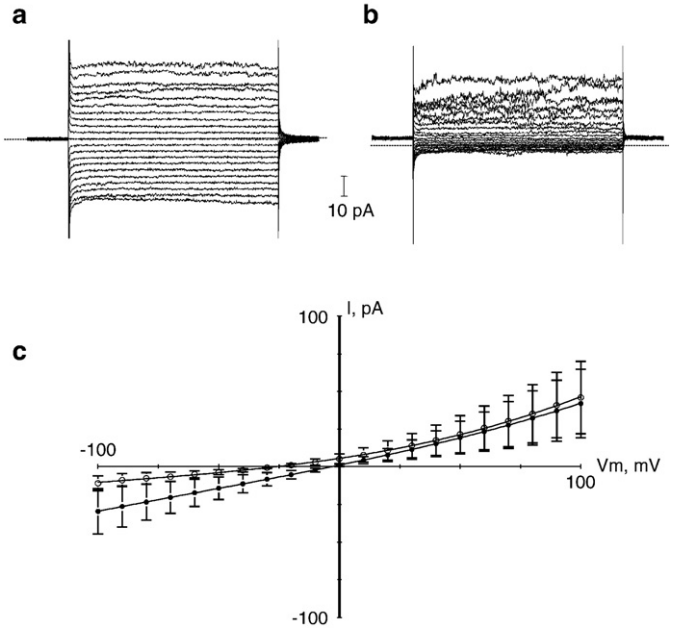

Fig. 1. Whole-cell recordings. Current traces recorded with Ringer solution (a) or with NMDG-Cl solution (b) bathing solutions, (voltage pulses between −100 and +100 mV, 10 mV increments, 500 ms). c. Corresponding *I*/*V* plots (mean ± SEM, 10 mV increments) from six cells in Ringer bathing solution (●) and the same 6 cells after replacement of cations by NMDG (○).

2.3. Current recordings

Characterization of single-channel currents was performed in the cell-attached and excised inside-out patch configurations. Single-channel currents were recorded by the method of Hamill (1983) using an RK400 patch-clamp amplifier (Biologic, Claix, France), filtered at 0.3 or 1 kHz (8 Pole Bessel filter, Kemo VBF8, France), digitized (48 kHz) and stored on a Digital Audio Tape (DTR 1204, Biologic). For analysis the data were played back and transferred to a computer and analyzed by the PAT computer program (Dempster, Strathclyde Electrophysiology Software v7.4). Patch pipettes (tip resistance ranging between 8 and 10 MΩ) were prepared from borosilicate glass capillaries (Clark Electromedical Instruments, England GC150F-10), pulled and polished on a horizontal programmable puller (DMZ, Werner Zeitz Augsburg, Germany). 5–10 GΩ seals were obtained by suctions of 10–25 kPa applied for less than 20 s. Under these conditions, the success rate of GΩ seal formation was 53%. The sign of the clamped voltage (V_p) refers to the pipette solution with respect to the bath and outward current (positive charges flowing across the patch membrane into the pipette) is shown as an upward deflection in the current traces. In the excised and cell-attached configuration the imposed membrane potential (V_m) is referred to $-V_p$. Current–voltage (*I*/*V*) curves were constructed by plotting the mean current amplitude for each clamped potential. Open probability (P_o) was determined as the fraction of digitized points above a threshold set midway between the closed and open peaks of current–amplitude histograms. P_o was determined from 180 s stable recordings. In these conditions, P_o was defined as the ratio of the total time spent in the open state to the total time of the complete record. Analyses were confined to patches showing one channel event histogram. Conventional 50% threshold analyses yielded distribution of dwell times that were fit by one or more exponential probability density functions consistent with multiple open and closed states. Because spontaneous patch excision often occurred, the recording of channel activity in the cell-attached mode was validated by demonstrable change in channel reversal potential and/or incidence upon excision.

Table 2
Summary of conductances and reversal potential values

Configuration	g [−60; E_r]	g E_r	g [+60; E_r]	E_r
Bath/pipette	pS	pS	pS	mV
Whole-cell				
$RnNa^+/K_{int}$ (n=75)	320±21	312±21	393±30	−2.3±0.6
RnK^+/K_{int} (n=6)	311±66	308±67	341±67	6.4±0.9
RCs^+/K_{int} (n=6)	468±187	430±130	503±182	7.2±3.7
$RnLi^+/K_{int}$ n=6)	214±51	259±60	351±69	−14.7±2.0*
$RnNMDG/K_{int}$ (n=6)	154±79	241±137	408±210	−26.4±5.5*

Mean values ± SEM of conductances calculated at the reversal potential (E_r), between E_r and −60 mV and between E_r and +60 mV, from whole-cell currents recorded using the patch-clamp technique in chicken red blood cells with different bathing and pipette-filling solutions.
*Changes are significantly different (P<0.05 unpaired t-test) as compared to the corresponding X/K_{int} values, with X standing for Na, K, Cs, Li or NMDG.

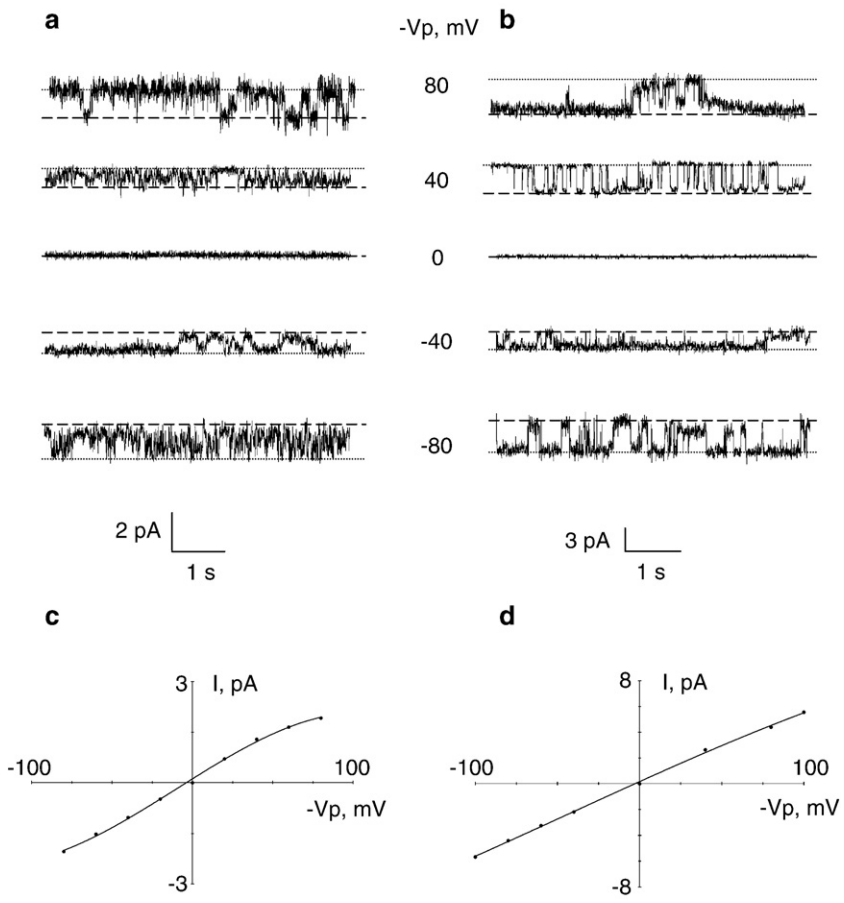

Fig. 2. Cell-attached recordings. a. and b. Representative records from single-channel currents of non-selective cation (NSC) channels in cell-attached patches at the indicated holding potentials. The bath contained isotonic Ringer solution and the pipettes were filled with 145 mM KCl pCa3 pipette solution. The closed state is shown by the dashed line. Downward deflection at negative clamp potentials indicates the flow of cations from pipette to cell interior. c. and d. Current/voltage relationships, under similar conditions to that of the upper traces.

Global currents were recorded in the fast-whole-cell, voltage-clamp mode, and 1-kHz low-pass-filtered by an RK400 amplifier (Biologic, Claix, France) using WCP software (WCP V3.2) and an CED 1401 Interface (Cambridge Electronic design, Cambridge, England). The whole-cell currents were evoked by a pulse protocol, clamping the voltage in twenty one successive 500 ms square pulses from the 0 mV holding potential, to potentials between −100 mV and +100 mV. The whole-cell configuration was assessed by increased membrane capacitance and reduction of access resistance to 3–5 MΩ. The original whole-cell current traces are depicted after 1 kHz low-pass filtering. The currents of the individual voltage square pulses are superimposed. The currents were analyzed by averaging the current between 100 and 400 ms of each voltage square pulse. The conductances were estimated for outward currents by linear regression between +20 mV and +80 mV voltage. The applied voltages refer to the cytoplasmic face of the membrane with respect to the extracellular space. The inward currents, defined as flow of positive charges from the extracellular medium to the cytoplasmic membrane face, are negative currents and depicted as downward deflections of the original current traces.

2.4. Liquid junction potentials

The liquid junction potential (LJP) was defined as the potential of the bath solution with respect to the pipette solution (Barry and Lynch, 1991) and the membrane potential (V_m) was calculated as $V_m = -V_p + \mathrm{LJP}$ where V_p is the reading provided by the patch-clamp amplifier. When bath solutions of different composition were successively applied to the patch membrane, the corresponding changes in liquid junction potentials were corrected using the Henderson equation (JPCalc computer program):

$$\mathrm{LJP} = RT/F \cdot S_f \cdot \ln \frac{\left(\sum_{i=1}^{n} z_i^2 \cdot u_i \cdot C_{p,i}\right)}{\left(\sum_{i=1}^{n} z_i^2 \cdot u_i \cdot C_{b,i}\right)}$$

where: $S_f = \dfrac{\left(\sum_{i=1}^{n} z_i \cdot u_i \cdot (C_{b,i} - C_{p,i})\right)}{\left(\sum_{i=1}^{n} z_i^2 \cdot u_i \cdot (C_{b,i} - C_{p,i})\right)}$ and u, C and z represent the mobility, concentration and valency of each ion species (i), and R, T and F are the gas constant, temperature and Faraday constant, respectively. Subscripts b and p denote bath and pipette solutions, respectively.

Data are presented as original recordings and as mean values ± SEM (n = number of observations). The paired Student's t-test was used for statistical analysis. A P value of <0.05 indicated statistical significance.

3. Results

In the presence of K_{int} pCa8 saline in the pipette and Ringer Na^+ in the bathing solution, only 40% of the attempts to achieve the whole-cell configuration were successful (139 out of 345 attempts). The seal resistance in these conditions was 4.0 ± 0.2 GΩ (n = 99), and the series resistance was 12.5 ± 0.2 MΩ (n = 99), which was offset at 80%.

In isosmotic condition with K_{int} pCa8 in the pipette and Ringer Na^+ saline in the bath, the current–voltage relationship was slightly outwardly rectified with a mean conductance (Gm) of 312±21 pS (n=75) and showed a reversal potential close to zero mV (E_r=−2.3±0.6 mV (n=75)) (Fig. 1a and c). Isosmotic replacement of sodium ions in the bathing solution by *N*-Methyl-D-Glucamine shifted the reversal potential toward the cations equilibrium (−26.4±5.5 mV (n=6, P<0.02), Fig. 1b and c) and reduced the inward currents by half (Gm=154±79 pS (n=6, P<0.002)) consistent with currents generated by cation movements. Furthermore, removal of extracellular chloride and replacement by gluconate neither change the reversal potential nor the membrane conductance (data not shown).

To characterize the permselectivity of the whole-cell cation currents recorded in isosmotic conditions, with K_{int} pCa8 in the pipette, Na^+ of the bath solution was replaced by various monovalent cations. Replacement of Na^+ by K^+, Cs^+, Li^+ in the bath solution did not change significantly the membrane conductance but significantly, albeit slightly, changed the reversal potential, giving a permselectivity ratio of Cs^+ (0.8±0.1; n=6) ≥ K^+ (1, n=6) ≥ Na^+ (1.5±0.1, n=6) > Li^+ (2.8±0.2, n=6) >> NMDG (6.0±1.6, n=6) (P<0.02; paired two-tailed t-test). The respective values of membrane conductances and reversal potentials are given in Table 2.

Fig. 2 depicts cell-attached recordings obtained after achieving a seal (Fig. 2a and b). As previously described two different cationic channel types were present in the membrane, but spontaneous activity was observed in less than 10% of records (564 seals out of 867 attempts). They could be distinguished by their unitary conductance.

The current current–voltage relationships were linear for both but for the first the conductance was 30.4 pS±3.3 pS (n=8) whereas it was 57.4±5.4 pS (n=8) for the second (Fig. 2c and d). In both cases, the reversal potential was close to zero (E_r=−1.7±2.3 mV, n=8 for the first, Fig. 2c, E_r=−2.9±1.4 mV, n=8 for the second), moreover neither the membrane conductances nor the reversal potentials were changed by replacement of sodium in the pipette by potassium indicating the non-selective cation nature of the currents recorded.

In a previous paper [11] we showed that one of the two cation channels present in the chicken red blood cell membrane is sensitive to membrane deformation. Here we have readdressed this question in whole-cell and inside-out configurations. However, since seal breakdown occurred frequently during suction in the cell-attached configuration, the stretch-activation of the channel was not tested in this configuration.

In the whole-cell configuration the membrane deformation was obtained by imposing calibrated positive pressure into the pipette under the control of a vacuometer allowing reproducible deformation for a given pipettes geometry. Fig. 3b shows the evolution of the ratio between the membrane conductance under a calibrated pressure and the membrane conductance in the absence of mechanical membrane deformation. A small increase in pressure was sufficient to induce a reversible increase in both inward and outward membrane conductances (Fig. 3a and b), suggesting that stretch stretch-activation is not voltage sensitive. The membrane conductance increased by 1.2±0.1 for 10^3 Pa applied but this change was not significant (P=0.53; paired, two-tailed Student's t-test, n=5). However, higher pressures induced

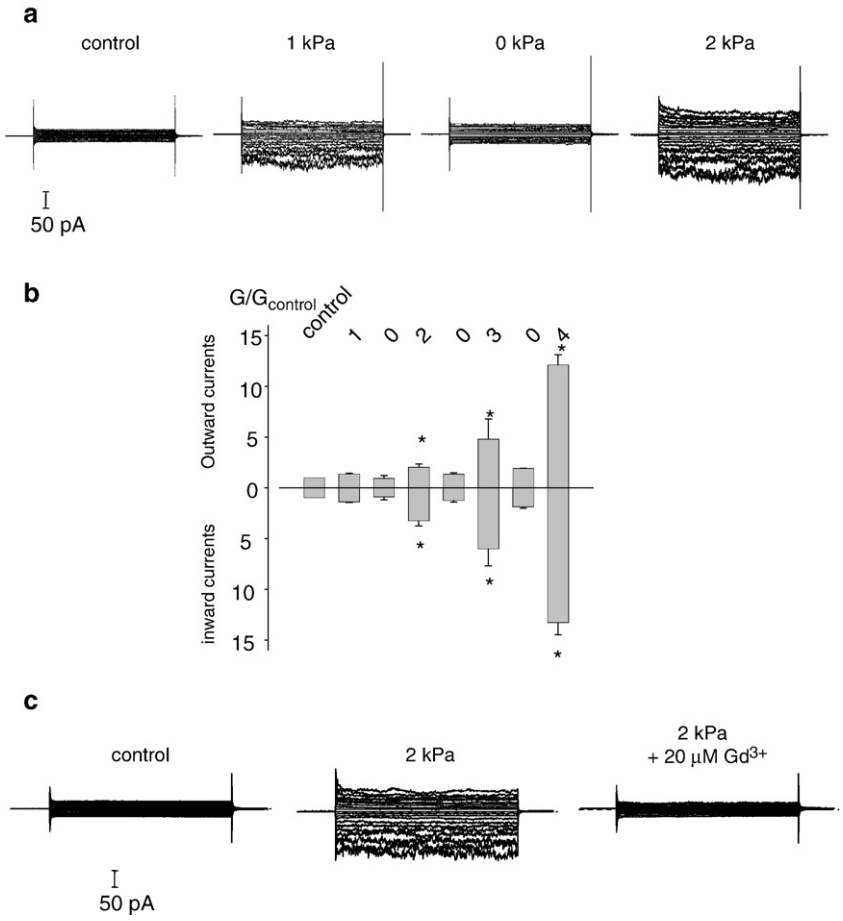

Fig. 3. Pressure activation of whole-cell currents. a. Representative recordings of reversible activation of membrane currents by positive pressure applied to the pipette obtained with Ringer in the bath and K_{int} pCa8 in the pipette. b. Changes in membrane conductance after application of positive pressure in the pipette, calculated as the ratio between the membrane conductance measured for a given pressure divided by the membrane conductance calculated when no pressure is applied (n=5). c. Representative recordings of the inhibition of the pressure activated currents by addition of 20 µM of Gd^{3+} (n=6).

significant changes in membrane currents. The membrane conductance increased by 2.3±0.3 for $2\cdot10^3$ Pa (n=12), by 4.5±1.3 for $3\cdot10^3$ Pa (n=5) and by 10.9±1.2 for $4\cdot10^3$ Pa (n=5) (P<0.05; paired, two-tailed Student's t-test). The nature of the currents induced by these mechanical deformations was assessed by the application of Gd^{3+} under $2\cdot10^3$ Pa tests. Addition of 20 μM of Gd^{3+}, reduced the membrane conductance to a level close to control (P=0.12; paired, two-tailed Student's t-test, n=10, Fig. 3c). However, the reversibility of the stretch-activation is only partial. Indeed, the currents measured after each cycle of membrane deformation, show a significant tendency to be greater than those measured during the former releases of pressure (P>0.05 for the third and fourth cycle of deformation).

The mechanosensitivity of the cationic currents observed in whole-cell configuration was further characterized by using the inside-out configuration of the patch-clamp technique. Indeed, due to the extreme fragility of seals in cell-attached configuration, depression in the patch pipette in most cases produced either a deterioration of seal resistance and appearance of leak rendering any further recordings impossible or a rupture of the piece of membrane into the pipette leading to the whole-cell configuration (assessed by bleaching of the cells seen under microscope). Nevertheless, once the inside-out configuration was achieved, application of depression on a quiescent patch induced channel activity. Even at a low depression such as $0.5\cdot10^3$ Pa, discrete channels opening were readily observed. However, at this depression, the current recorded corresponded only to a substate (1/3 of the full opening) and the full opening was only observed in rare cases. Nevertheless, full opening of the channel was usually observed with 10^3 Pa and above. The P_o values, measured at a given membrane potential, were clearly related to the intensity of the depression imposed on the membrane patch. The open probability values at different pressures were fitted by nonlinear regression using equation for a sigmoidal shape according to the equation $y=a/(1+\exp(-(x-x_0)/b))$, where y is the open probability calculated as P_o/P_o max, a is the maximal P_o/P_o max ratio, x is the sampling pressure, x_0 is essentially the pressure at half activation ($P_{1/2}$=2.1 kPa), and b represents the variability of cells in the population (Fig. 4a and b). This activation was reversible in 90% of the cells tested so far. Once activated, the unitary conductance of the channel established with Ringer in the pipette and with K_{int} pCa8 in the bathing solution was 22.0±2.5 pS (n=11) and the reversal potential was close to zero mV (0.3±1.1 mV, n=11). Using KCl (145 mM) in the pipette did not change the membrane conductance, but 1:1 dilution of the bathing solution by half shifted the reversal potential toward the Nernst equilibrium for cations (E_r=+17.3±1.3 mV (n=7)), giving a permselectivity ratio of P_{cation}/P_{anion} of 179±68 (n=7). Moreover, this NSC channel was inhibited by addition of Gd^{3+} (20 μM) in the bathing solution (data not shown).

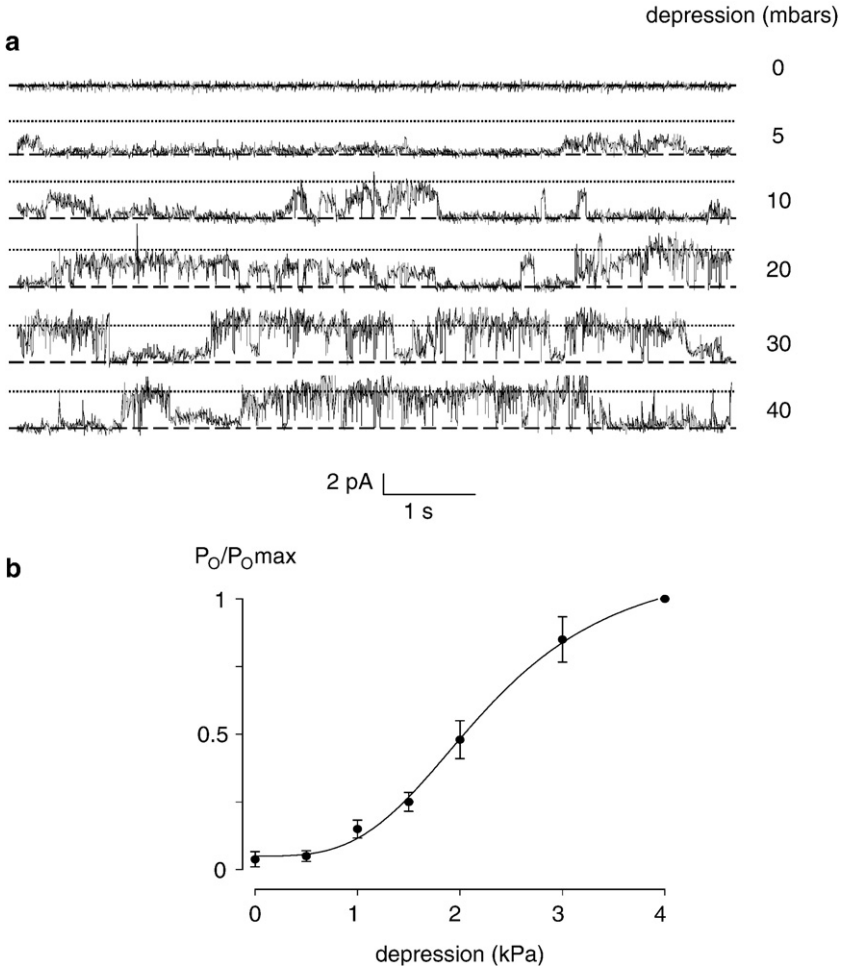

Fig. 4. Stretch-activation of NSC channels. a. Single-channel current recordings performed in inside-out configuration from a patch presenting no spontaneous channel activity and after application of calibrated suction (0.5 to 4 kPa) producing reversible activation of NSC channels. b. Changes in open probability after application of membrane deformation, calculated as the ratio P_o/P_o max determined with a depression of 4 kPa (mean±SEM, n=6). When the NSC channel activity was induced by suction, the P_o value, measured at a membrane potential of +60 mV was clearly related to the intensity of the depression imposed on the membrane patch (n=6).

The second NSC channel observed in cell-attached configuration presents also a very low spontaneous frequency of openings. However, we have previously shown that one of the cation channel present in the chicken red blood cell membrane can be activated by the rise of intracellular calcium concentration. Some of these types of channels can also be activated by increasing the intracellular concentration of cyclic nucleotides. In whole-cell configuration, addition of 8Br-cAMP, a cell permeable analogue of the cAMP, at a concentration of 1 mM increased the membrane current in a time-dependent manner. The current was multiplied by 7.4±1.8 (n=6) Fig. 5. The maximum current was reached after 20–25 min of incubation. This cAMP-dependent current was inhibited by flufenamic acid (0.1 mM) (Fig. 5b).

In inside-out configuration cAMP was added to the bathing solution (K_{int}) when rare openings could be observed. Addition of 1 mM induced a rapid increase (<30 s) of the open probability (Fig. 6b). Fig. 6a shows typical traces recorded at different membrane potential after addition of 1 mM cAMP. The corresponding current–voltage relationship (Fig. 6c) was similar to the I/V curves obtained after stimulation by intracellular calcium [11], signifying that it probably corresponded to activation of the same channel type.

In the excised inside-out configuration with 145 mM KCl (K_{int}) in the bath and 145 mM KCl in the pipette, the current–voltage relationship showed a reversal potential (E_r) of 1.4±2.0 mV (n=6). The channel slope conductance was 71.1±6.6 pS between E_r and 60 mV (Fig. 6c). Substitution of NaCl for KCl in the pipette or substitution of Na_{int} for K_{int} in the bath did not significantly change the conductance over this voltage range. The cationic versus anionic selectivity was determined by dilution of the bathing solution KCl from 145 mM (K_{int}) to 72.5 mM (K_{int} 1/2). The I/V relationship showed a right shift and E_r was 17.2±0.7 mV (n=6, KCl in the pipette), close to the Nernst equilibrium potential for cations (17.5 mV). The relative permeability P_{cation}/P_{cl}-derived from the GHK relation was 76±12 (n=6). These results are supported by experiments where E_r shifted to 24.5±3.1 mV (n=4) when Na^+ or K^+ were replaced by NMDG in the bathing solution (Fig. 4b). The apparent P_K/P_{NMDG} ratio was 3.9±0.8 (n=4) which is consistent with our previous report that chicken RBC membranes possess a significant permeability for large cations such as choline via non-selective permeable cation channel. One of the hypotheses of the role of the up-regulation of the non-selective cation channels during infection by *Plasmodium gallinaceum* was to counteract the cell volume increase. Hence we tested this hypothesis by submitting cells to hyposmotic challenge. Changes in osmolarity (180 mosM) were able to produce an increase of membrane conductance, indicating possible involvement of such channels in response to volume challenge (Fig. 7). In this case, in spite of a difference of pharmacology between the two channels (Gd^{3+} or flufenamic acid sensitivity), it was impossible to establish which one was the first to be open after hyposmotic shock, indicating that probably a strong interaction between the two channels exist.

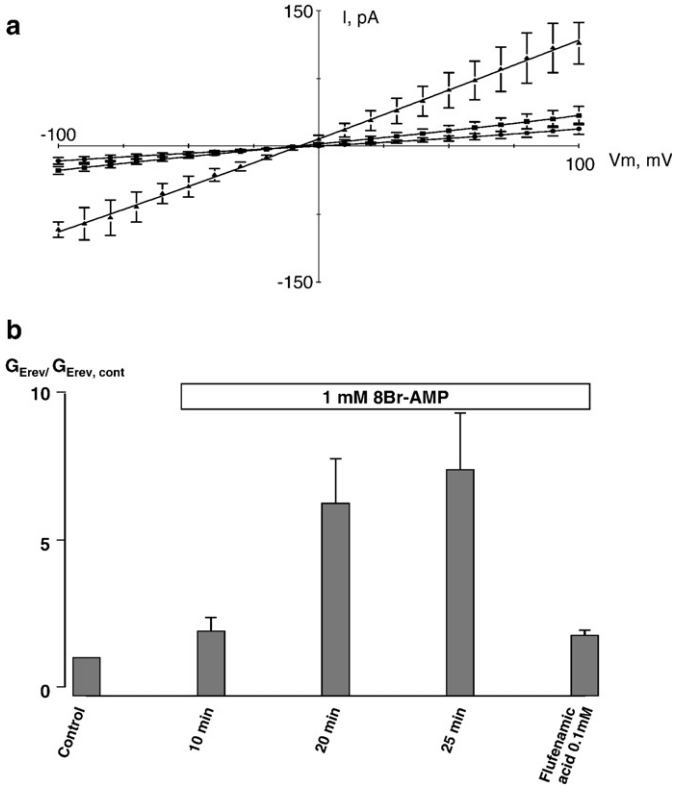

Fig. 5. Activation of NSC currents by cyclic nucleotides in whole-cell configuration. a. Current/voltage relationships of membrane currents recorded before (●), 25 min after addition to the bathing solution of 1 mM of 8Br-cAMP (▲) and after addition of 0.1 mM of flufenamic acid (■). Data are expressed as mean±SEM (n=6) b. Changes in membrane conductances calculated as the ratio between the membrane conductance before (control) and after addition of 8Br-cAMP (10, 20 and 25 min) and following inhibition of these currents by flufenamic acid (n=6).

4. Discussion

In a previous study, using the patch-clamp technique we demonstrated that chicken red cell membranes are endowed with cation channels that may be activated after infection by the parasite *P. gallinaceum* [11]. Here we readdressed the characterization of membrane currents and non-selective cation channels in non-infected cells. Using the whole-cell configuration we could demonstrate that the membrane conductance is generated by cation channels and that two different types of cation channels can account for the whole-cell membrane conductance.

The first channel described in this study displays the common features of the stretch-activated channels described in the literature. Indeed in symmetrical concentrations of NaCl the channel presents a unitary conductance of 22 pS, which is in good agreement with the values reported for stretch-activated non-selective cation channels permeant for calcium in red blood cells [3,23] or some other cell types [26–29]. Moreover, here we demonstrate that this channel is highly sensitive to mechanical deformation either in whole-cell or inside-out configuration. Most reports (review in [30]) show that depression above 2 kPa is needed to activate such channel type whereas in the present study depression as low as 0.5 kPa was sufficient to induce channel activity. Although this channel type presents some common feature with the non-selective cation channel present in the human red blood cell membrane (conductance, permeability to Ca^{2+}), it does probably not belong to the same family. The non-selective cation channels responsible for the whole-cell membrane currents are not dependent of extracellular chloride (shown by the absence of increase of membrane currents after substitution of chloride by gluconate), indicating that they are also not voltage-dependent. This NSC channel was shown to conduct Ca^{2+} [11] and calcium permeation is a feature of stretch-activated cation non-selective channels in endothelial cells [31], choroids plexus epithelium [32], oocytes [33–36] and renal proximal tubule [37]. In view of the large selectivity of the NSC channel for calcium, its role could be to permit permeation of Ca^{2+} ions which could activate calcium-dependent processes such as cell volume regulation in most cells. Here a decrease in bath osmolarity enhances the membrane cation currents indicating an involvement of this channel type after cell volume challenge.

The second channel type reported in this study was also partially described in a previous paper, where its sensitivity to the rise of intracellular calcium was shown [11]. One of the common features of the non-selective cation channel activated by calcium is to be activated by an increase in intracellular concentration of nucleotide too [38,39]. This channel is thought to be up-regulated in

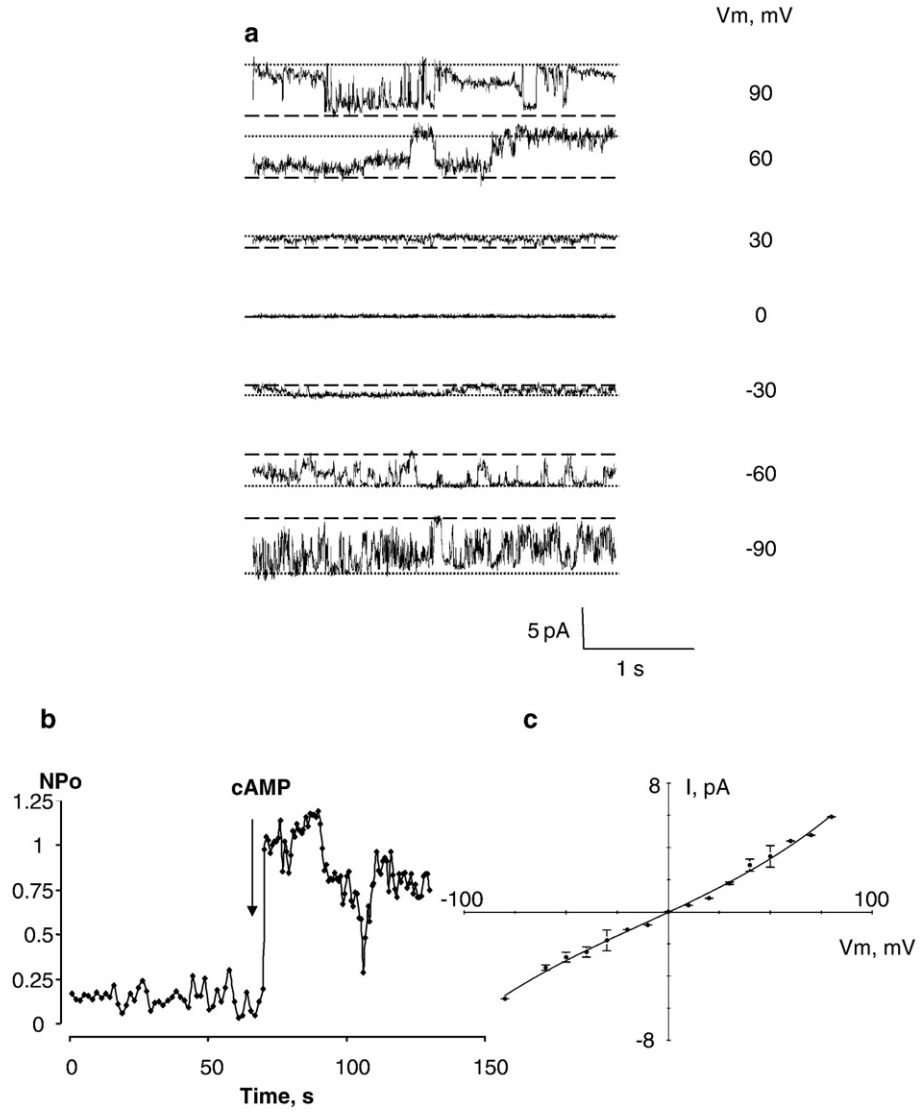

Fig. 6. Activation of NSC currents by cyclic nucleotides in inside-out configuration. a. Typical current traces obtained in inside-out configuration at different membrane potential after addition to the bathing solution of 1 mM of cAMP on a quiescent patch. b. Changes in open probability (NP_o) measured after addition of 1 mM of cAMP on the cytosolic face of a quiescent patch where two channels were present. c. Current–voltage relationship obtained in inside-out configuration with K_{int} pCa8 in the bath and 1 mM cAMP. Data presented are the mean±SEM of 6 different cells.

P. gallinaceum infected cells [11], and the relative permeability of this channel to large impermeant cations like NMDG (this study) correlated to the permeability to choline [11] may suggest that during infection this channel may be a route to supply the parasite with this precursor needed to synthesize membranes.

Cation channels play a key role in erythrocytes cell death [40,41], and disease where non-regulated cation leak lead to cell shrinkage [6,42]. This work confirms that comparative studies of nucleated red cells provide good models for elucidating these processes and disorders and to identify the molecular nature of the cation channels involved.

References

[1] J.S. Gibson, A.R. Cossins, J.C. Ellory, Oxygen-sensitive membrane transporters in vertebrate red cells, J. Exp. Biol. 203 (Pt 9) (2000) 1395–1407.
[2] F. Garcia-Romeu, A.R. Cossins, R. Motais, Cell volume regulation by trout erythrocytes: characteristics of the transport systems activated by hypotonic swelling, J. Physiol. 440 (1991) 547–567.
[3] S. Egee, F. Lapaix, A.R. Cossins, S.L. Thomas, The role of anion and cation channels in volume regulatory responses in trout red blood cells, Bioelectrochemistry 52 (2000) 133–149.
[4] A. Baroin, F. Garcia-Romeu, T. Lamarre, R. Motais, A transient sodium-hydrogen exchange system induced by catecholamines in erythrocytes of rainbow trout, *Salmo gairdneri*, J. Physiol 356 (1984) 21–31.
[5] C. Brugnara, Therapeutic strategies for prevention of sickle cell dehydration, Blood Cells Mol. Diseases 27 (2001) 71–80.
[6] V.L. Lew, R.M. Bookchin, Ion transport pathology in the mechanism of sickle cell dehydration, Physiol. Rev. 85 (2005) 179–200.
[7] J.A. Browning, H.M. Staines, H.C. Robinson, T. Powell, J.C. Ellory, J.S. Gibson, The effect of deoxygenation on whole-cell conductance of red blood cells from healthy individuals and patients with sickle cell disease, Blood 109 (2007) 2622–2629.
[8] K. Kirk, K.J. Ashworth, B.C. Elford, R.A. Pinches, J.C. Ellory, Characteristics of 86Rb+ transport in human erythrocytes infected with *Plasmodium falciparum*, Biochim. Biophys. Acta 1061 (1991) 305–308.
[9] H.M. Staines, C. Rae, K. Kirk, Increased permeability of the malaria-infected erythrocyte to organic cations, Biochim. Biophys. Acta 1463 (2000) 88–98.
[10] H.M. Staines, J.C. Ellory, K. Kirk, Perturbation of the pump-leak balance for Na^+ and K^+ in malaria-infected erythrocytes, Am. J. Physiol., Cell Physiol. 280 (2001) C1576–C1587.
[11] S.L. Thomas, S. Egee, F. Lapaix, L. Kaestner, H.M. Staines, J.C. Ellory, Malaria parasite *Plasmodium gallinaceum* up-regulates host red blood cell channels, FEBS Lett. 500 (2001) 45–51.
[12] C. Duranton, S. Huber, V. Tanneur, K. Lang, V. Brand, C. Sandu, F. Lang, Electrophysiological properties of the *Plasmodium falciparum*-induced cation conductance of human erythrocytes, Cell. Physiol. Biochem. 13 (2003) 189–198.
[13] H. Godart, J.C. Ellory, KCl cotransport activation in human erythrocytes by high hydrostatic pressure, J. Physiol. 491 (1996) 423–434.

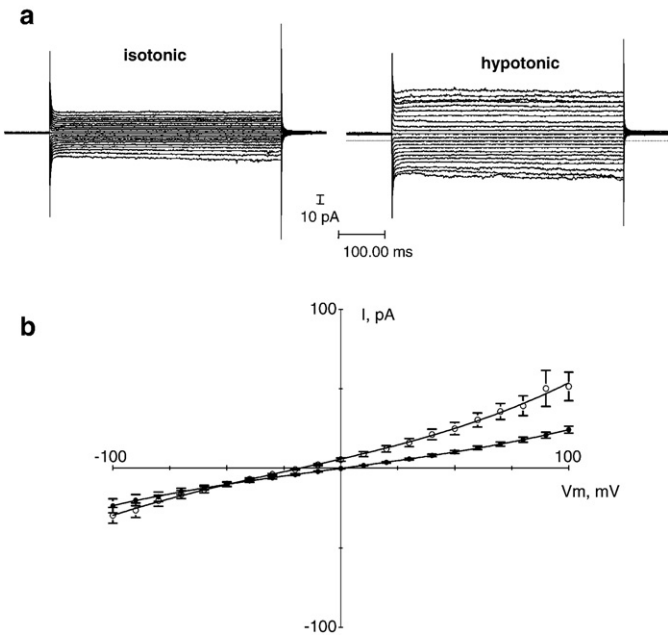

Fig. 7. Activation in whole-cell configuration of NSC current by hypotonic shock. a. Typical recordings of activation of membrane currents by hypotonic shock (180 mosM). b. Current–voltage relationship obtained in whole-cell configuration with K_{int} pCa8 in the pipette before (●) and after hyposmotic shock (○). Data presented are the mean ± SEM of 6 different cells.

[14] P.W. Flatman, J. Creanor, Regulation of Na^+–K^+–$2Cl^-$ cotransport by protein phosphorylation in ferret erythrocytes, J. Physiol. 517 (1999) 699–708.
[15] I. Bernhardt, A.Y. Bogdanova, D. Kummerow, K. Kiessling, J. Hamann, J.C. Ellory, Characterization of the K^+ (Na^+)/H^+ monovalent cation exchanger in the human red blood cell membrane: effects of transport inhibitors, Gen. Physiol. Biophys. 18 (1999) 119–137.
[16] S. Thomas, S. Egee, Fish red blood cells: characteristics and physiological role of the membrane ion transporters, Comp. Biochem. Physiol., Part A Mol. Integr. Physiol. 119 (1998) 79–86.
[17] P. Bennekou, The feasibility of pharmacological volume control of sickle cells is dependent on the quantization of the transport pathways. A model study, J. Theor. Biol. 196 (1999) 129–137.
[18] V.B. Brand, C.D. Sandu, C. Duranton, V. Tanneur, K.S. Lang, S.M. Huber, F. Lang, Dependence of *Plasmodium falciparum* in vitro growth on the cation permeability of the human host erythrocyte, Cell. Physiol. Biochem. 13 (2003) 347–356.
[19] P. Christophersen, P. Bennekou, Evidence for a voltage-gated, non-selective cation channel in the human red cell membrane, Biochim. Biophys. Acta 1065 (1991) 103–106.
[20] P. Bennekou, The voltage-gated non-selective cation channel from human red cells is sensitive to acetylcholine, Biochim. Biophys. Acta 1147 (1993) 165–167.
[21] L. Kaestner, C. Bollensdorff, I. Bernhardt, Non-selective voltage-activated cation channel in the human red blood cell membrane, Biochim. Biophys. Acta 1417 (1999) 9–15.
[22] L. Kaestner, P. Christophersen, I. Bernhardt, P. Bennekou, The non-selective voltage-activated cation channel in the human red blood cell membrane: reconciliation between two conflicting reports and further characterisation, Bioelectrochemistry 52 (2000) 117–125.
[23] S. Egee, O. Mignen, B.J. Harvey, S. Thomas, Chloride and non-selective cation channels in unstimulated trout red blood cells, J. Physiol. 511 (1998) 213–224.
[24] F. Lapaix, S. Egee, L. Gibert, G. Decherf, S.L. Thomas, ATP-sensitive K^+ and Ca^{2+}-activated K^+ channels in lamprey (*Petromyzon marinus*) red blood cell membrane, Pflugers Arch. 445 (2002) 152–160.
[25] C. Duranton, S.M. Huber, F. Lang, Oxidation induces a Cl-dependent cation conductance in human red blood cells, J. Physiol. 539 (2002) 847–855.
[26] T.H. Yeh, M.C. Tsai, S.Y. Lee, M.M. Hsu, P. Tran Ba Huy, Stretch-activated nonselective cation, Cl^- and K^+ channels in apical membrane of epithelial cells of Reissner's membrane, Hear. Res. 109 (1997) 1–10.
[27] T.H. Yeh, P. Herman, M.C. Tsai, P. Tran Ba Huy, T. Van den Abbeele, A cationic nonselective stretch-activated channel in the Reissner's membrane of the guinea pig cochlea, Am. J. Physiol. 274 (1998) C566–C576.
[28] Y. Marunaka, Y. Shintani, G.P. Downey, N. Niisato, Activation of Na^+-permeant cation channel by stretch and cyclic AMP-dependent phosphorylation in renal epithelial A6 cells, J. Gen. Physiol. 110 (1997) 327–336.
[29] O. Christensen, E.K. Hoffmann, Cell swelling activates K^+ and Cl-channels as well as nonselective, stretch-activated cation channels in Ehrlich ascites tumor cells, J. Membr. Biol. 129 (1992) 13–36.
[30] O.P. Hamill, Twenty odd years of stretch-sensitive channels, Pflugers Arch. 453 (2006) 333–351.
[31] J.B. Lansman, T.J. Hallam, T.J. Rink, Single stretch-activated ion channels in vascular endothelial cells as mechanotransducers? Nature 325 (1987) 811–813.
[32] O. Christensen, Mediation of cell volume regulation by Ca^{2+} influx through stretch-activated channels, Nature 330 (1987) 66–68.
[33] C. Methfessel, V. Witzemann, T. Takahashi, M. Mishina, S. Numa, B. Sakmann, Patch clamp measurements on *Xenopus laevis* oocytes: currents through endogenous channels and implanted acetylcholine receptor and sodium channels, Pflugers Arch. 407 (1986) 577–588.
[34] V. Taglietti, M. Toselli, A study of stretch-activated channels in the membrane of frog oocytes: interactions with Ca^{2+} ions, J. Physiol. 407 (1988) 311–328.
[35] W.J. Moody, M.M. Bosma, A nonselective cation channel activated by membrane deformation in oocytes of the ascidian *Boltenia villosa*, J. Membr. Biol. 107 (1989) 179–188.
[36] X.C. Yang, F. Sachs, Block of stretch-activated ion channels in *Xenopus* oocytes by gadolinium and calcium ions, Science 243 (1989) 1068–1071.
[37] D. Filipovic, H. Sackin, A calcium-permeable stretch-activated cation channel in renal proximal tubule, Am. J. Physiol. 260 (1991) F119–F129.
[38] S. Wu, T.M. Moore, G.H. Brough, S.R. Whitt, M. Chinkers, M. Li, T. Stevens, Cyclic nucleotide-gated channels mediate membrane depolarization following activation of store-operated calcium entry in endothelial cells, J. Biol. Chem. 275 (2000) 18887–18896.
[39] A.L. Eguiguren, J. Rios, N. Riveros, F.V. Sepulveda, A. Stutzin, Calcium-activated chloride currents and non-selective cation channels in a novel cystic fibrosis-derived human pancreatic duct cell line, Biochem. Biophys. Res. Commun. 225 (1996) 505–513.
[40] F. Lang, K.S. Lang, P.A. Lang, S.M. Huber, T. Wieder, Mechanisms and significance of eryptosis, Antioxid. Redox Signal. 8 (2006) 1183–1192.
[41] K.S. Lang, P.A. Lang, C. Bauer, C. Duranton, T. Wieder, S.M. Huber, F. Lang, Mechanisms of suicidal erythrocyte death, Cell. Physiol. Biochem. 15 (2005) 195–202.
[42] P. Bennekou, L. de Franceschi, O. Pedersen, L. Lian, T. Asakura, G. Evans, C. Brugnara, P. Christophersen, Treatment with NS3623, a novel Cl-conductance blocker, ameliorates erythrocyte dehydration in transgenic SAD mice: a possible new therapeutic approach for sickle cell disease, Blood 97 (2001) 1451–1457.